World Academy of Science, Engineering and Technology
International Journal of Materials and Metallurgical Engineering
Vol:10, No:2, 2016

Thermophysical and Heat Transfer Performance of Covalent and Noncovalent Functionalized Graphene Nanoplatelet-Based Water Nanofluids in an Annular Heat Exchanger

Hamed K. Arzani, Ahmad Amiri, Hamid K. Arzani, Salim Newaz Kazi, Ahmad Badarudin

Abstract**—**The new design of heat exchangers utilizing an annular distributor opens a new gateway for realizing higher energy optimization. To realize this goal, graphene nanoplatelet-based water nanofluids with promising thermophysical properties were synthesized in the presence of covalent and noncovalent functionalization. Thermal conductivity, density, viscosity and specific heat capacity were investigated and employed as a raw data for ANSYS-Fluent to be used in two-phase approach. After validation of obtained results by analytical equations, two special parameters of convective heat transfer coefficient and pressure drop were investigated. The study followed by studying other heat transfer parameters of annular pass in the presence of graphene nanopleteles-based water nanofluids at different weight concentrations, input powers and temperatures. As a result, heat transfer performance and friction loss are predicted for both synthesized nanofluids.

Keywords**—**Heat transfer, nanofluid, turbulent flow, forced convection flow, graphene nanoplatelet.

I. Introduction

NANOFLUID is defined as a new kind of fluid comprises different nanoparticles, which suspended in liquid molecules. Heat transfer of nanofluid can be functions of dimension, properties, volume concentration of nanoparticles etc. According to the experimental investigations, nanofluids have shown a significant potential for augmentation of energy transfer and also higher thermal conductivities in comparison to the base fluids. Owing to the nanofluid characteristics, many kinds of industries including automotive radiator systems, computer processing cooling equipment, home heating and cooling appliances, and power plant cooling systems can employ the suggested technique.

Recently a majority of developments in industrial technology are focused on the energy optimization as well as the reduction of system processing time. Consequently, in the field of heat transfer, the request to increase in cooling capacities has been vital for these compact thermal systems. The conventional methods for example use of extension surfaces like fins or utilization of microchannels with high heat transfer surface are to obtain the desired high cooling efficiency. On the other hand, the cooling fluid characteristics have been taken under consideration.

The single-phase or two-phase approaches could be applied in simulating convective heat transfer by nanofluid. The single-phase method assumes that nanoparticles and base fluid move with the same velocity and they are in thermal equilibrium, so this method is easier and needs less computational time. But it is important and notable to find applicable equations which compute properties of single-phase nanofluids. However, the single-phase method has been employed in a number of numerical researches of convective heat transfer by nanofluids [1]–[8]. In general, the single-phase approach and experimental results have not good agreement, due to lack of appropriate equations for predicting both nanoparticles and basefluid, implying the low extent of validation in results and lack of realizing nanofluids properties. Also, some nanofluid parameters such as dispersibility, sedimentation, Brownian motion of nanoparticles in basefluids, Brownian forces, volume or weight concentration of solid particles in basefluids may influence nanofluid flow regime and heat transfer rate. Therefore, the slip velocity between nanoparticles and basefluid must be considered for simulating nanofluid flows and/or heat transfer [9]. Due to Brownian movement of particles in basefluids, two-phase approach opens a new gateway for introducing the main characteristics of nanofluids, indicating a good agreement with theoretical and experimental results [10], [11]. Various multiphase approaches have been presented to predict and describe behaviour of complex flows. Numerous multiphase flow studies used the theory of interacting continua or the “Mixture Theory” [12]–[15]. This method works based on the underlying theory that each phase can be mathematically defined as a continuum.

Lotfi et al. [16] employed single-phase, two-phase Eulerian and two-phase mixture approaches to simulate flow behaviour in the presence of nanofluids through a straight pipe. They concluded that two phase mixture method has more accurate results than the other two approaches. Some investigators have used this approach to simulate the behaviour of nanofluids [4], [5], [17]–[19]. Mirmasoumi and Behzadmehr [18] and Akbarinia and Laur [5] considered the influence of nanoparticle size on nanofluid flow in a horizontal pipe. Also, the annular tube and/or heat exchanger are a common and unique geometry in industrial applications and specially heat

Hamed K. Arzani, Ahmad Amiri, S.N. Kazi are with the Department of Mechanical Engineering, University of Malaya, Kuala Lumpur, Malaysia (e-mail: hamedarzani@outlook.com; ahm.amiri@gmail.com or ahm.amiri@siswa.um.edu.my; salimnewaz@ um.edu.my).

transfer equipment. They attracted a large number of scientists and have been employed in different equipment such as electronic devices, air condition and ventilation systems, turbo machinery, nuclear reactors, gas turbines, and double pipe heat exchanger. So, the investigation of heat transfer in annular heat exchangers and introducing novel method for improving their performance play a vital role in energy-saving [20]–[22].

Abu-Nada et al. [22] investigated heat transfer rate of annular heat exchanger in the presence of Al_2O_3-based water nanofluid with single phase method. They considered different thermal conductivity and viscosity models to evaluate heat transfer improvement in the annular heat exchanger. Izadi et al. [21] have also simulated laminar forced convection of Al_2O_3-based water nanofluid in a two dimensional annular heat exchanger with the single-phase method.

The objective of the present study is abstracted in the synthesizing new kind of fluid, graphene nanopleteles-based water nanofluids at different weight concentrations, the experimental investigation of thermophysical properties of covalent and non-covalent nanofluids (GNP-SDBS- and GNP-COOH-based water nanofluids) and numerical simulation of annular heat exchanger in the presence of prepared nanofluids. To realize this goal appropriately, two-phase is employed. The comparison of analytical and proposed result by simulation in two-phase method confirmed the validity of work. Then, the nanofluids flow in a two dimensional annular pipe investigated in different weight concentrations and ratio of heat flux. As a result, Nusselt number profiles and friction factor are measured for both synthesized nanofluids.

II. Methodology

A. Covalent Functionalization of GNP

To provide non-covalent nanofluids (GNP-SDBS-based water nanofluid) with known weight concentrations, the given amount of pristine GNP was first weighted, followed by pouring a weight ratio SDBS/pristine GNP of 0.5:1 into a vessel filled with the given distillated water.

Regarding covalent nanofluid (GNP-SDBS-based water nanofluid), based on the technique explained by Wang et al. [33] with slight modification, carboxylation of GNP was performed. In order to generate carboxylated GNP, the GNP (1 g) with a mixture of HNO_3 and H_2SO_4 (1:3 volume ratio) was first sonicated for 0.5 h at room temperature in a closed vessel. Then, the GNP suspension was poured into a Teflon reaction vessel and placed in an industrial microwave (Milestone MicroSYNTH programmable microwave system) with output power of 700 W and heated up to 90 °C for 15 minutes. The resulting suspension was cooled at room temperature and then diluted with 200 mL deionized water to reduce the power of acids for filtration. The GNP suspension was filtered through 45 μm polytetrafluoroethylene (PTFE) membrane, and the filtrate was continually washed with the deionized water to remove any unreacted acids. The functionalized sample was dried overnight at 40°C in a vacuum. Then, the GNP-COOH produced after microwave phase was dispersed in the deionized water at room temperature. Dispersed concentration of 0.1 wt.% was easily obtained in water in the presence of COOH groups on the surface of GNPs.

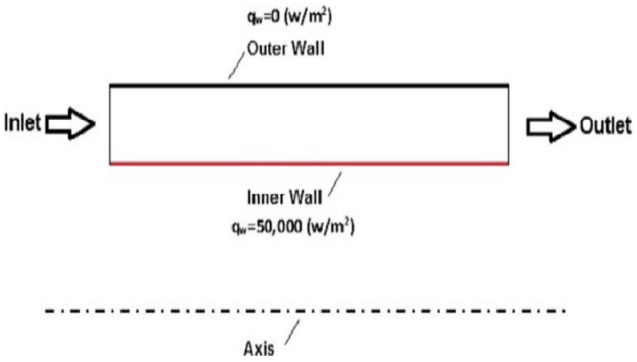

Fig. 1 2D geometrical configuration of annular channel

B. Geometry and Mesh Structure

This study is focused on a horizontal annulus formed between an inner heat generating solid circular cylinder and an outer isothermal cylindrical boundary undergoing turbulent convection nanofluid flow. An annular tube in the horizontal position with diameter of d and lengths of L is simulated in the present study. A two-dimensional (2D) geometry has been selected for being investigated. Fig. 1 shows the geometrical configuration taken under study.

The inlet and outlet positions of the tube, profiles of uniform axial velocity (V_0), constant temperature (T_0=35°C) and different Reynolds numbers, are illustrated in Fig. 2.

The meshing tool available in ANSYS was used to construct the computational mesh. A structured mesh based on a rectangular grid was used throughout the domain. Several grid distributions had been tested and the results were compared to ensure that the calculated results were grid independent. Fig. 3 draws the comparison of Nusselt numbers versus the Reynolds numbers for water as a working fluid at three different grid distributions. It has shown that obtained results are independent of the number of grid points.

To reduce computational time and effort, the total grid points and the elements have employed in the whole tube are 16,441 and 16,000, respectively. A non-uniform grid was used in the meshing step, close to the wall grids as smaller to get better results. (Fig. 4).

C. Simulation Cases and Boundary Conditions

A constant heat flux of 50,000 (W/m^2) is applied at the tube wall. The influence of weight fraction of nanoparticles in the range of 0 to 0.1% and the Reynolds number (Re) on the convective heat transfer is investigated. The pressure outlet boundary condition is considered.

D. Numerical Methods

The numerical method available in the commercial CFD package of ANSYS-Fluent, V15 has been used here. Fluent uses a finite volume approach to convert the governing partial differential equations into a system of discrete algebraic equations. As the discretization methods, a second-order

upwind scheme is selected for the momentum, turbulent kinetic energy and turbulent dissipation rate equations whereas the first order upwind for energy equation is selected. For two-phase calculations, the phase momentum equations with the shared pressure are solved in a coupled and segregated fashion. The phase coupled SIMPLE (PC-SIMPLE) algorithm is employed for the pressure–velocity coupling. PC-SIMPLE is an extension of the SIMPLE algorithm to multiphase flows. The under-relaxation factors were set to 0.3 except for energy (set to 1) to speed up the convergence. The scaled residuals for the velocity components and energy are set equal to 10^{-8} and 10^{-9}, respectively.

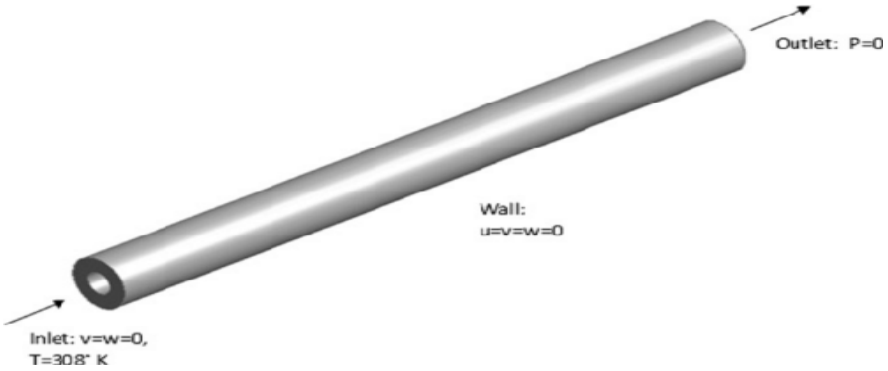

Fig. 2 Boundary conditions for the tube

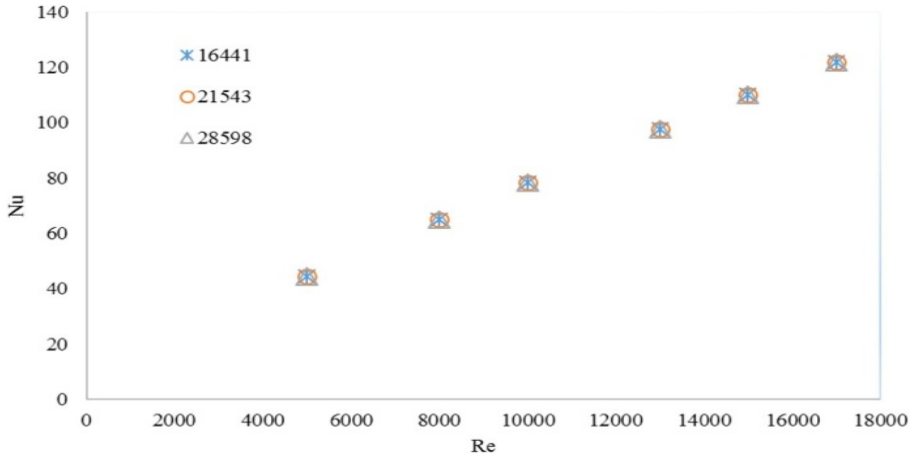

Fig. 3 Comparison of Nusselt numbers versus Reynolds numbers for water at three different grid distributions

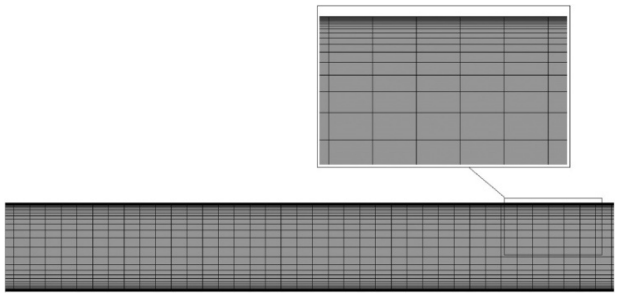

Fig. 4 Mesh configuration of annular channel

Considering the turbulent forced convection in a steady flow of an incompressible and Newtonian fluid, the governing equations can be written as follows [23]:

a) Continuity equation

$$\nabla.\left(\rho_{eff}\overline{V}\right)=0 \tag{1}$$

b) Momentum equations

$$\nabla.(\rho_{eff}\overline{V}\overline{V})=-\nabla\overline{P}+\mu_{eff}\nabla^{2}\overline{V}-\rho_{eff}\nabla.(\overline{v'v'}) \tag{2}$$

c) Conservation of energy

$$\nabla.(\rho_{eff}C_{p,eff}\overline{V}\overline{T})=\nabla.((\mathrm{k}_{eff}+\mathrm{k}_{t})\nabla\overline{T}) \tag{3}$$

In the above equations, the symbols $\overline{V}$, $\overline{P}$ and $\overline{T}$ represent the time averaged flow variables, while the symbol v′ represents the fluctuations in velocity. The term in the momentum equations $\rho_{eff}\nabla.(\overline{v'v'})$ represents the turbulent shear stress. The terms of k_{eff} and k_t represent the effective molecular conductivity and the turbulent thermal conductivity, respectively.

TABLE I
THE EFFECTIVE PHYSICAL PROPERTIES OF THE (GNP-SDBS/WATER) AND (GNP-COOH/WATER) NANOFLUIDS AT DIFFERENT MASS FRACTIONS

	Water	GNP-SDBS/Water			GNP-COOH/Water		
		0.025%	**0.05%**	**0.1%**	**0.025%**	**0.05%**	**0.1%**
Density, ρ (kg/m³)	994.1	995.115	996.88	998.16	994.95	995.9	996.88
Specific heat, cp (J/kg.K)	4178	4152.66	4104.07	4055.95	4164.5	4111.1	4056.68
Thermal conductivity, k (W/m.K)	0.623	0.645	0.675	0.695	0.685	0.71	0.75
Dynamic viscosity, μ (Ns/m²)	0.0007	0.0010	0.0011	0.0013	0.0008	0.0009	0.001

To model flow in the turbulent regime, the standard k-ε model can be employed based on the Launder and Spalding study [24], which is as follow:

$$\nabla.(\rho_{eff} kV) = \nabla.[(\frac{\mu_t}{\sigma_k})\nabla(k)] + G_k - \rho_{eff}\varepsilon \quad (4)$$

$$\nabla.(\rho_{eff} \varepsilon V) = \nabla.[\frac{\mu_t}{\sigma_\varepsilon}\nabla\varepsilon] + \frac{\varepsilon}{k}(C_{1\varepsilon}G_k - C_{2\varepsilon}\rho_{eff}\varepsilon) \quad (5)$$

$$G_k = \mu_t(\nabla V + (\nabla V)^T),\ \mu_t = \rho_{eff} C_\mu \frac{k^2}{\varepsilon} \quad (6)$$

$$C_\mu = 0.09, \sigma_k = 1.00, \sigma_\varepsilon = 1.30, C_{1\varepsilon} = 1.44, C_{2\varepsilon} = 1.92 \quad (7)$$

where μ_{eff} and μ_t are the effective viscosity of nanofluid and coefficient of viscosity in turbulent regime, respectively.

The thermophysical properties of water, GNP-SDBS- and GNPCOOH-based water nanofluids are presented in Table I.

E. Validation Results

A horizontal annulus formed between an inner heat generating solid circular cylinder and an outer isothermal cylindrical boundary undergoing turbulent convection water flow is used for the numerical study.

At the inlet, temperature was set up to 308°K and the tube wall was exposed to 50,000 (W/m^2), which was uniform. The numerical analyses were performed at various Reynolds numbers up to 1000 iterations until the calculated results reached to steady state.

The comparison of the temperature profiles predicted by the analytical equations and ANSYS model is shown in Fig. 5. It can be seen that the validity of results obtained by ANSYS is reasonable. The temperature has been calculated via the formula nearly overlapping with the outcomes from the fluent. The analytical solutions for the straight tube have been obtained by (8):

$$Tm(x) = Tm_i + (\frac{q \times p}{\dot{m} \times C_p})x \quad (8)$$

The Nusselt number has been calculated by the fluent and the analytical solutions, which the comparison between analytical results and ANSYS results are presented in Fig. 6. The Nusselt numbers are obtained in the region of fully developed flow which has almost coincided with the values from the Gnielinski correlation with the maximum error of 6.3%. As a result, the numerical output by the ANSYS-fluent is in good agreement with analytical once for both graphene-based water nanofluids in an annular heat exchanger.

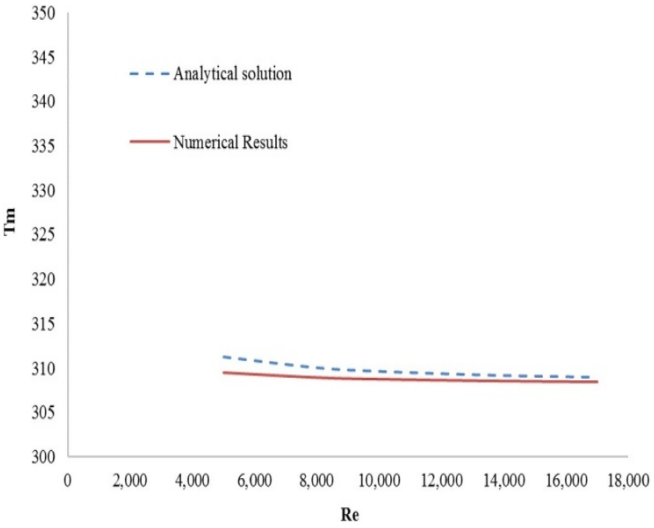

Fig. 5 Temperature profiles in the straight tube and the comparison between analytical and numerical results

TABLE II
DYNAMIC VISCOSITY OF THE GNP-SDBS AND GNP-COOH-BASED WATER NANOFLUIDS AS THE FUNCTIONS OF TEMPERATURE AND WEIGHT CONCENTRATION AT SHEAR RATE OF 140 S^{-1}

Temp.	Water	GNP-SDBS/Water			GNP-COOH/Water		
		0.025%	**0.05%**	**0.1%**	**0.025%**	**0.05%**	**0.1%**
20	0.001002	0.0013	0.0014506	0.0015478	0.0010961	0.0011494	0.0012166
35	0.000761	0.00100985	0.0011418	0.0012785	0.0008407	0.0008639	0.0009264
50	0.000557	0.000789185	0.0009397	0.001118	0.0006293	0.0006757	0.0007313
65	0.000441	0.0006635	0.0008001	0.0009831	0.0004781	0.0005244	0.0006032
80	0.000353	0.000547265	0.000647	0.000835	0.000358	0.000406	0.000457

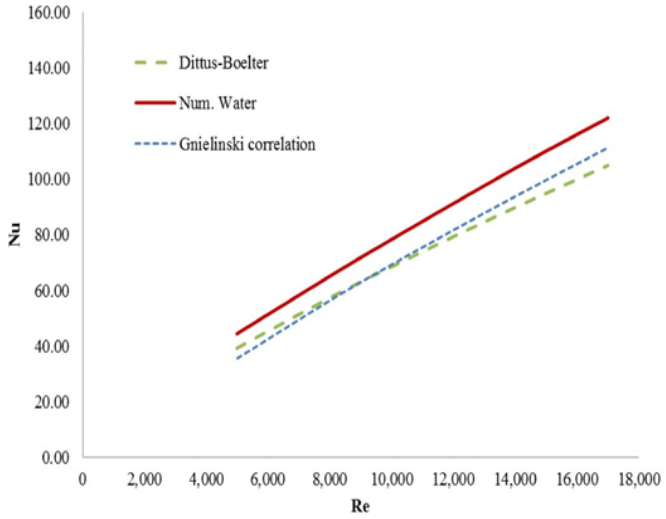

Fig. 6 Nusselt profiles for various Reynolds numbers through annular heat exchanger obtained by numerical two-phase method and its comparison with Gnielinski and Dittus–Boelter equations

III. Results and Discussions

A. Thermophysical Properties

The viscosities of GNP-SDBS- and GNP-COOH-based water nanofluids were investigated for different temperatures and concentration, as can be observed in Table II. Similar to other coolants, the rheological behavior of GNP-SDBS and GNP-COOH-based water nanofluids show two significant characteristics: (i) an enhancement in the viscosity with increasing concentration, and (ii) a decrease in viscosity with increasing temperature, which is due to weakening of the intermolecular forces of the particles and fluid itself. It can be seen that the enhancement in the viscosity of both synthesized nanofluids is not similar with the increase in weight concentration, which obtained by higher viscosity of SDBS. In addition, in agreement with [25], [27] and [26], viscosity decreases with increase in temperature.

Also, the densities of GNP-SDBS- and GNP-COOH-based water nanofluids are investigated as the functions of temperature and weight concentration, which are shown in Table III.

TABLE III
Densities of the GNP-SDBS- and GNP-COOH-Based Water Nanofluids for Different Concentrations

T °C	Water	GNP-SDBS/Water			GNP-COOH/Water		
		0.025 %	**0.05%**	**0.1 %**	**0.025 %**	**0.05 %**	**0.1 %**
20	0.998	0.998	0.999	0.999	0.998	0.998	0.99966
30	0.995	0.996	0.997	0.998	0.996	0.997	0.99835
40	0.992	0.993	0.995	0.997	0.993	0.994	0.99543
50	0.984	0.988	0.989	0.991	0.989	0.990	0.98878

Consist with the results, the density of GNP-SDBS- and GNP-COOH-based water nanofluids declines by increasing the temperature, which can be related to the enhancement in the volume of the liquid with enhancing the temperature. There is an upward trend between the density of GNP-SDBS- and GNP-COOH-based water nanofluids and their weight concentration.

Table IV shows the thermal conductivities of GNP-SDBS- and GNP-COOH-based water nanofluids as the functions of temperature and concentration. One can clearly see that the thermal conductivity of GNP-SDBS- and GNP-COOH-based water nanofluids is higher than that of water. Also, it can be seen that a higher increase in the thermal conductivity of GNP-SDBS- and GNP-COOH-based water nanofluids as compared with water with respect to the temperature. Thus, it confirms that fluid temperature plays a key role in increasing the thermal conductivity of GNP-SDBS- and GNP-COOH-based water nanofluids. In comparison with water, the main mechanism of thermal conductivity enhancement with respect to the temperature is attributed to the Brownian motion of the nanoparticles suspended in the base-fluid, which is a dominating function of temperature [26], [27]. For basefluids comprising of GNP, the formation of surface nanolayers plays an important role in dominating of energy transfer. Liquid molecules can generate layers around the GNP, thereby enhancing the local ordering of the liquid layer at the interface region. Thus, the liquid layer at the interface would rationally comprise a higher thermal conductivity than the basefluid [27], [28], which announces the critical duty of creating nanolayer in increasing thermal conductivity of GNP-SDBS- and GNP-COOH-based water nanofluids.

TABLE IV
Thermal Conductivity of the GNP-SDBS- and GNP-COOH-Based Water Nanofluids for Different Concentrations

T °C	Water	GNP-SDBS/Water			GNP-COOH/Water		
		0.025 %	**0.05 %**	**0.1 %**	**0.025 %**	**0.05 %**	**0.1 %**
20	0.582	0.61	0.63	0.65	0.63	0.66	0.69
30	0.601	0.63	0.66	0.68	0.67	0.69	0.73
40	0.624	0.66	0.69	0.71	0.7	0.73	0.778
50	0.642	0.68	0.7	0.73	0.73	0.76	0.81

The influence of temperature in a range of 25 to 65°C as well as weight concentration of GNP on the specific heat capacity of GNP-WEG coolant was also studied in this study. Table V shows that an increase in the weight concentrations of GNP-SDBS- and GNP-COOH-based water nanofluids caused a drop in the specific heat capacity, but is insignificant.

TABLE V
The Specific Heat Capacity of the GNP-SDBS- and GNP-COOH-Based Water Nanofluids for Different Concentrations

T °C	Water	GNP-SDBS/Water			GNP-COOH/Water		
		0.025%	**0.05%**	**0.1%**	**0.025%**	**0.05%**	**0.1%**
20	4.1814	4.1524	4.1037	4.0553	4.1642	4.1103	4.0563
30	4.1800	4.1528	4.1041	4.0560	4.1649	4.1112	4.05693
40	4.1791	4.1524	4.1039	4.0558	4.1640	4.1109	4.05644
50	4.1800	4.1527	4.1040	4.0559	4.1647	4.1105	4.05667

B. Numerical Study

The numerical study on the turbulent forced convection flow of non-covalent nanofluid (GNP-SDBS-based water nanofluids) and covalent nanofluid (GNP-COOH-based water nanofluid) in an annular tube has been performed at various

Reynolds numbers and weight concentrations. There are 48 cases of simulations where weight concentration of 0%, 0.025%, 0.05%, and 0.1% and the Reynolds numbers of 5000, 8000, 10,000, 13,000, 15,000 and 17,000 have been selected.

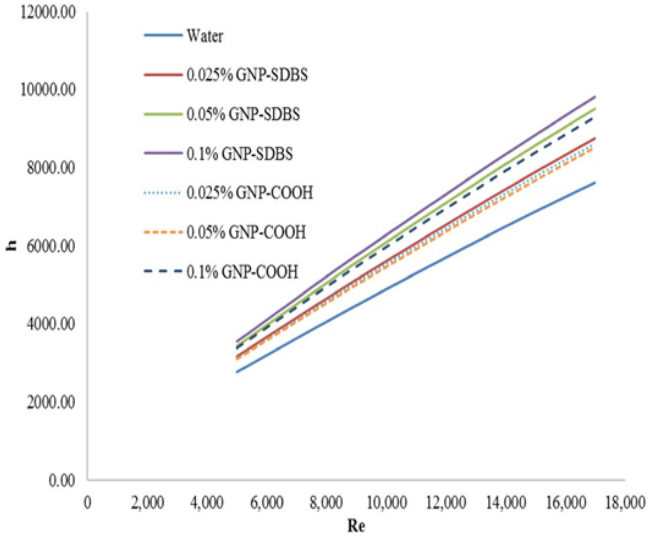

Fig. 7 Average heat transfer coefficients for various Reynolds numbers

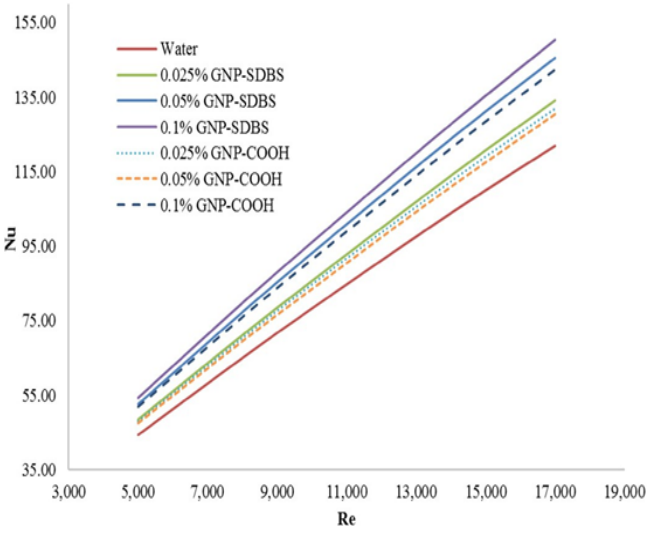

Fig. 8 Average Nusselt numbers for various Reynolds numbers

Figs. 7 and 8 respectively presented the convective heat transfer coefficients and the average Nusselt numbers of pure water, GNPSDBS- and GNP-COOH-based water nanofluids as a function of the Reynolds number. One can be seen some lines with different slopes, which increased with increase in Reynolds number as well as concentration of both type of GNPs. This phenomenon can be attributed to the higher thermal conductivity of basefluid in the presence of GNPs. For example, about 22% increase in the convective heat transfer coefficient is obtained at Reynolds number of 17,000 in the presence of 0.1 wt.% of GNP-SDBS.

The friction factor at different Reynolds number and weight concentrations of GNP-SDBS and GNP-COOH are shown in Fig. 9. It can be seen that the friction factor decreases with increasing the Reynolds number and/or volume flow rate at different concentrations. The friction factor also increases as the concentration of GNP increases in both samples comprised GNP-SDBS and GNP-COOH and the minimum value of friction factor is indicated for the basefluid. Also, as the Reynolds number increases, friction factor dependence of the concentration is not changed, implying more similarity to which for water. It is obvious that Brownian motion plays an essential role in momentum transfer between the nanoparticles and base-fluid molecules at low Reynolds numbers, resulting in an enhancement in the friction factor than that of the base-fluid [29]-[32]. However, this mechanism cannot be dominant at high Reynolds numbers. In summary, the viscosity of working fluid does not play a key role in decreasing the friction factor at high Reynolds numbers and velocity can be considered as the most important parameter in increasing the friction factor compared with the base-fluid.

The friction factor at different Reynolds number and weight concentrations of GNP-SDBS and GNP-COOH as different axial positions are shown in Fig. 10. The extent of friction factor remains constant throughout the tube.

C. Pressure Drop

Fig. 11 shows the measured pressure drop at different Reynolds numbers and concentrations of nanofluids. As shown in Fig. 11, as the inlet velocity and concentration of nanofluids increases, the pressure drop increases. The pressure drops for GNP-COOH/water nanofluids at various concentrations are not quit close to that for water pressure drop. This observation confirms that the effect of GNP concentration on the viscosity of nanofluids and consequently on the pressure drop is significant, especially in the presence of GNP-SDBS. On the other hand, as the concentration of GNP-SDBS increases, the variation of pressure drop with the Reynolds number shows sharper slope. That is, the GNP-SDBS/water nanofluid at the mass fraction of 0.1% and Reynolds number of 17,000 shows the maximum pressure drop. Expectedly, the viscosity curve and pressure drop curves present similar trends in the presence of covalent and non-covalent samples, which can be caused from the direct connection between viscosity and pressure drop.

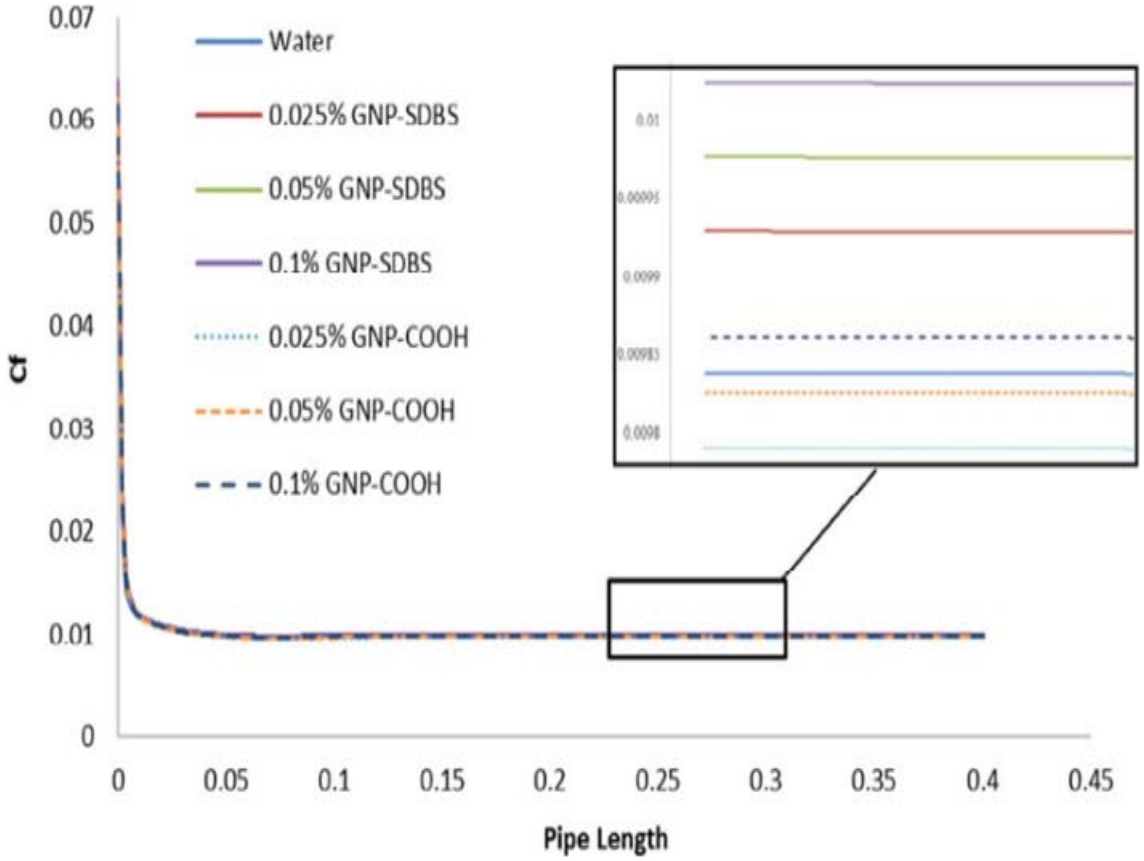

Fig. 9 Friction factor for various Reynolds numbers

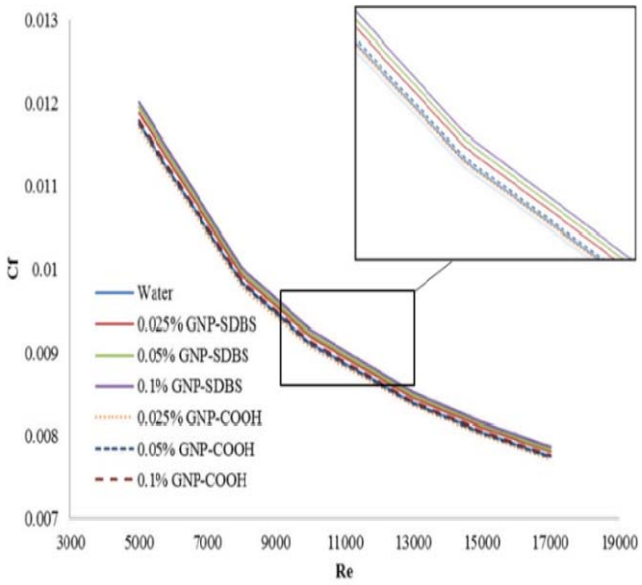

Fig. 10 Friction factor throughout the tube for different concentrations of GNP-SDBS and GNP-COOH

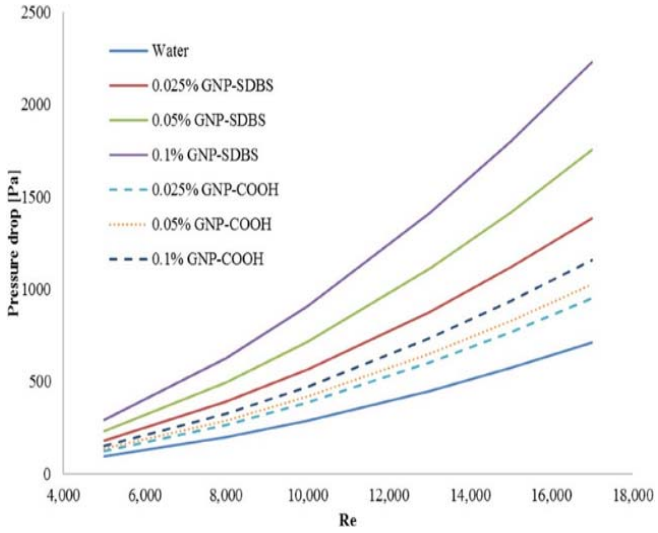

Fig. 11 Relation between pressure drops along the annulus at various Reynolds numbers for different concentrations

IV. Conclusion

Here, thermophysical studies of new kind of coolant have been investigated in the presence of GNP-SDBS as a noncovalent component and GNP-COOH as a covalent component. The results of thermal conductivity, density, viscosity and specific heat capacity are introduced. Thermophysical properties of both nanofluids along with two-

phase modelling via ANSYS open a new gateway for investigation of convective heat transfer coefficient and pressure drop. Heat transfer enhancement of non-covalent nanofluid (GNP-SDBS-based water nanofluid) and covalent nanofluid (GNP-COOH-based water nanofluid) in an annular heat exchanger has been considered in the presence of CFD two-phase mixture model. The validation results confirmed the applicability of Fluent to simulate heat transfer phenomena in the presence of GNP nanofluids. The main conclusions gained are as follows:

- The suspended GNP-SDBS and GNP-COOH nanoparticles significantly enhance the heat transfer performance of the base fluid.
- The increase in GNP concentration resulted in an increase in the thermal conductivity rate.
- At constant concentration, the higher Reynolds number means the higher Nusselt number, implying higher heat transfer rate in the presence of nanofluids including GNP.
- The extent of friction factor is also declined as the Reynolds number increases.
- An increase in GNP concentration leads to an increase in friction factor.
- Throughout the tube, the amount of friction factor changed insignificantly.

REFERENCES

[1] B. Barbés, R. Páramo, E. Blanco, C. Casanova, Thermal conductivity and specific heat capacity measurements of CuO nanofluids, J. Therm. Anal. Calorim. 115 (2) (2014) 1883–1891.
[2] G. Roy, C.T. Nguyen, P.-R. Lajoie, Numerical investigation of laminar flow and heat transfer in a radial flow cooling system with the use of nanofluids, Superlattice. Microst. 35 (3) (2004) 497–511.
[3] K. Khanafer, K. Vafai, M. Lightstone, Buoyancy-driven heat transfer enhancement in a two-dimensional enclosure utilizing nanofluids, Int. J. Heat Mass Transf. 46 (19) (2003) 3639–3653.
[4] A. Akbarinia, A. Behzadmehr, Numerical study of laminar mixed convection of a nanofluid in horizontal curved tubes, Appl. Therm. Eng. 27 (8) (2007) 1327–1337.
[5] A. Akbarinia, R. Laur, Investigating the diameter of solid particles effects on a laminar nanofluid flow in a curved tube using a two phase approach, Int. J. Heat Fluid Flow 30 (4) (2009) 706–714.
[6] F. Talebi, A.H. Mahmoudi, M. Shahi, Numerical study of mixed convection flows in a square lid-driven cavity utilizing nanofluid, Int. Commun. Heat Mass Transfer 37 (1) (2010) 79–90.
[7] M. Shahi, A.H. Mahmoudi, F. Talebi, Numerical study of mixed convective cooling in a square cavity ventilated and partially heated from the below utilizing nanofluid, Int. Commun. Heat Mass Transfer 37 (2) (2010) 201–213.
[8] L.S. Sundar, K. Sharma, Turbulent heat transfer and friction factor of Al_2O_3 nanofluid in circular tube with twisted tape inserts, Int. J. Heat Mass Transf. 53 (7) (2010) 1409–1416.
[9] Y. Xuan, Q. Li, Heat transfer enhancement of nanofluids, Int. J. Heat Fluid Flow 21 (1) (2000) 58–64.
[10] A. Amiri, M. Shanbedi, H. Yarmand, H.K. Arzani, S. Gharehkhani, E. Montazer, R. Sadri, W. Sarsam, B. Chew, S. Kazi, Laminar convective heat transfer of hexylamine-treated MWCNTs-based turbine oil nanofluid, Energy Convers. Manag. 105 (2015) 355–367.
[11] M. Shanbedi, D. Jafari, A. Amiri, S.Z. Heris, M. Baniadam, Prediction of temperature performance of a two-phase closed thermosyphon using artificial neural network, Heat Mass Transf. 49 (1) (2013) 65–73.
[12] M. Manninen, V. Taivassalo, S. Kallio, On the Mixture Model for Multiphase Flow, Technical Research Centre of Finland, 1996.
[13] L.M. Crowe, D.S. Reid, J.H. Crowe, Is trehalose special for preserving dry biomaterials? Biophys. J. 71 (4) (1996) 2087.
[14] M. Ishii, Thermo-fluid dynamic theory of two-phase flow, NASA STI/Recon Technical Report A, 75 1975, p. 29657.
[15] H.-K. Xu, Viscosity approximation methods for nonexpansive mappings, J. Math. Anal. Appl. 298 (1) (2004) 279–291.
[16] R. Lotfi, Y. Saboohi, A. Rashidi, Numerical study of forced convective heat transfer of nanofluids: comparison of different approaches, Int. Commun. Heat Mass Transfer 37 (1) (2010) 74–78.
[17] V. Bianco, F. Chiacchio, O. Manca, S. Nardini, Numerical investigation of nanofluids forced convection in circular tubes, Appl. Therm. Eng. 29 (17) (2009) 3632–3642.
[18] S. Mirmasoumi, A. Behzadmehr, Effect of nanoparticles mean diameter on mixed convection heat transfer of a nanofluid in a horizontal tube, Int. J. Heat Fluid Flow 29 (2) (2008) 557–566.
[19] S. Mirmasoumi, A. Behzadmehr, Numerical study of laminar mixed convection of a nanofluid in a horizontal tube using two-phase mixture model, Appl. Therm. Eng. 28 (7) (2008) 717–727.
[20] E. Abu-Nada, H.F. Oztop, Effects of inclination angle on natural convection in enclosures filled with Cu–water nanofluid, Int. J. Heat Fluid Flow 30 (4) (2009) 669–678.
[21] M. Izadi, A. Behzadmehr, D. Jalali-Vahida, Numerical study of developing laminar forced convection of a nanofluid in an annulus, Int. J. Therm. Sci. 48 (11) (2009) 2119–2129.
[22] E. Abu-Nada, Z. Masoud, A. Hijazi, Natural convection heat transfer enhancement in horizontal concentric annuli using nanofluids, Int. Commun. Heat Mass Transfer 35 (5) (2008) 657–665.
[23] T.M. Shih, Numerical Heat Transfer, CRC Press, 1984.
[24] B.E. Launder, D. Spalding, The numerical computation of turbulent flows, Comput. Methods Appl. Mech. Eng. 3 (2) (1974) 269–289.
[25] G.H. Ko, K. Heo, K. Lee, D.S. Kim, C. Kim, Y. Sohn, M. Choi, An experimental study on the pressure drop of nanofluids containing carbon nanotubes in a horizontal tube, Int. J. Heat Mass Transf. 50 (23 –24) (2007) 4749–4753.
[26] A. Amiri, R. Sadri, M. Shanbedi, G. Ahmadi, B. Chew, S. Kazi, M. Dahari, Performance dependence of thermosyphon on the functionalization approaches: an experimental study on thermo-physical properties of graphene nanoplatelet-based water nanofluids, Energy Convers. Manag. 92 (2015) 322–330.
[27] S.S.J. Aravind, P. Baskar, T.T. Baby, R.K. Sabareesh, S. Das, S. Ramaprabhu, Investigation of structural stability, dispersion, viscosity, and conductive heat transfer properties of functionalized carbon nanotube based nanofluids, J. Phys. Chem. C 115 (34) (2011) 16737–16744.
[28] N. Jha, S. Ramaprabhu, Synthesis and thermal conductivity of copper nanoparticle decorated multiwalled carbon nanotubes based nanofluids, J. Phys. Chem. C 112 (25) (2008) 9315 –9319.
[29] M. Shanbedi, A. Amiri, S. Rashidi, S.Z. Heris, M. Baniadam, Thermal performance prediction of two-phase closed thermosyphon using adaptive neuro-fuzzy inference system, Heat Transfer Eng. 36 (3) (2015) 315–324.
[30] A. Amiri, R. Sadri, G. Ahmadi, B. Chew, S. Kazi, M. Shanbedi, M. Sadat Alehashem, Synthesis of polyethylene glycol-functionalized multi-walled carbon nanotubes with a microwave-assisted approach for improved heat dissipation, RSC Adv. 5 (45) (2015) 35425–35434.
[31] A. Amiri, R. Sadri, M. Shanbedi, G. Ahmadi, S. Kazi, B. Chew, M.N.M Zubir, Synthesis of ethylene glycol-treated Graphene Nanoplatelets with one-pot, microwave assisted functionalization for use as a high performance engine coolant, Energy Convers. Manag. 101 (2015) 767 – 777.
[32] K. Solangi, S. Kazi, M. Luhur, A. Badarudin, A. Amiri, R. Sadri, M.N.M. Zubir, S. Gharehkhani, K. Teng, A comprehensive review of thermo-physical properties and convective heat transfer to nanofluids, Energy 89 (2015) 1065 –1086.
[33] Y. Wang, Z. Iqbal, S. Mitra, Rapidly functionalized, water-dispersed carbon nanotubes at high concentration, J. Am. Chem. Soc. 128 (1) (2006) 95 –99.